A Thermodynamic Equation of State for n-Butane[1]

Hiroyuki Miyamoto[2,3] and Koichi Watanabe[2]

[1] Paper presented at the Fourteenth Symposium on Thermophysical Properties, June 25-30, 2000, Boulder, Colorado, U.S.A.

[2] Department of System Design Engineering, Faculty of Science and Technology, Keio University, 3-14-1, Hiyoshi, Kohoku-ku, Yokohama 223-8522, Japan.

[3] Author to whom correspondence should be addressed.

ABSTRACT

We developed a Helmholtz free energy equation of state for the fluid phase of n-butane (R-600) on the basis of new temperature scale of ITS-90. This model has been established on the basis of selected measurements of the pressure-density-temperature (P, ρ, T), isochoric heat capacity, speed of sound and the saturation properties. Three sets of supplementary calculated values from the ancillary correlations regarding the saturation vapor-pressures, saturated vapor- and liquid-densities were added to the input data. The linear structural regression optimization and nonlinear fitting procedure were used to determine the functional form and the numerical parameters of the present equation of state. Throughout our graphical comparison with available experimental data, it is recognized that the developed model enables to represent most of the reliable experimental data accurately in the range of validity covering temperatures from 134.87 K (the triple point temperature) to 589 K, pressures up to 69 MPa, and densities up to 745 $kg{\cdot}m^{-3}$, respectively. The smooth behaviors of the derived thermodynamic properties have also been confirmed in the entire fluid phase of n-butane

KEY WORDS: equation of state; Helmholtz free energy; hydrocarbon; natural working fluid; n-butane; R-600; refrigerant; thermodynamic property.

1. INTRODUCTION

The hydrocarbon (HC) refrigerants are recognized to be attractive substances to consist several promising alternative mixtures for refrigeration and air-conditioning systems because of their zero ODP and negligible GWP values. By blending them with nonflammable hydrofluorocarbon (HFC) refrigerants, the flammability of HCs and larger GWP values of HFCs would have been reduced simultaneously. If their flammability issue is solved in any advanced refrigeration-based systems, the HC refrigerants including propane (R-290), n-butane (R-600), iso-butane (R-600a), and their mixtures may also become promising.

Having such a background mentioned above taken into account, the accurate thermodynamic equations of state for pure HCs and pure HFCs have to be demanded for developing the thermodynamic property models of their mixtures. The accurate equations of state for pure HFCs have recently been available, including the fundamental equations of state formulated in terms of a nondimensional Helmholtz free energy for R-32, R-134a and R-143a by Tillner-Roth and Yokozeki [1], Tillner-Roth and Baehr [2], and Lemmon and Jacobsen [3], respectively, which all were accepted as the international standard equations of state by the IEA(International Energy Agency)-Annex XVIII. Regarding the HCs, a Helmholtz free energy model for R-290 has also been developed by the present authors [4] on the basis of available updated experimental data. As a continuation, in the present study, we aimed to formulate an accurate Helmholtz-type thermodynamic model for the entire fluid phase of R-600.

Among the available thermodynamic models for R-600, the model by Younglove and Ely [5] has widely been used in various applications including the REFPROP (Ver. 6.01) [6]. However, it was developed based upon the available experimental data by the middle of the 1980's and old temperature scale, IPTS-68. Recently, several new measurements on $P\rho T$, caloric and acoustic properties for R-600 became available and therefore we considered it worthwhile to propose a new model on the basis of these new

sets of experimental data and new temperature scale, ITS-90, for the development of the thermodynamic formulations for the HFC mixtures with R-600.

2. AVAILABLE EXPERIMENTAL DATA

We collected about 2000 experimental thermodynamic property measurements for R-600. A summary of the data in the single-phase region such as $P\rho T$, caloric and acoustic property measurements, and that of saturation property data including vapor pressures, saturated vapor- and liquid-densities, liquid heat capacities and speeds of sound are listed in Table I. Most of experimental thermodynamic property data reported prior to 1982 were summarized by Haynes and Goodwin [23]. For our modeling, the temperature values of all experimental data are converted to ITS-90, except a set of $P\rho T$ property data in the vapor phase by Gupta and Eubank [11], isochoric heat capacities in the liquid phase by Magee and Lüddecke [12], and a set of saturated-liquid heat capacities by Magee and Lüddecke [12] that all have been published recently.

In the single-phase region, three sets of experimental $P\rho T$ property data by Olds et al. [9], Haynes [10], and Gupta and Eubank [11], which are given with # in Table I, were mainly used as input data. The other sets of $P\rho T$ data were always used only to compare their reproducibility with the developed formulation; the data by Beattie et al. [7], and a set of data by Kay [8] which include a large quantity of calculated values extrapolated from the original measurements by the author [8]. Regarding the caloric and acoustic properties, three sets of experimental measurements which contain a set of isochoric heat capacity, C_V, data by Magee and Lüddecke [12], and two sets of speed of sound, W, data by Niepmann [14] and Ewing et al. [15] were also used as input data. The experimental isobaric heat capacity, C_P, data by Sage et al. [13] were not used as input data.

The saturation property data used for our modeling are also given with # in Table I. Regarding the saturation vapor-pressures, P_S, saturated vapor- and liquid-densities, ρ''

and ρ', these selected data were used to prepare three sets of supplementary input data calculated from the ancillary correlations discussed in the next section. The saturated-liquid heat capacity, $C_.$, data by Magee and Lüddecke [12] and saturated-liquid speed of sound, W', data by Niepmann [14] were directly used as additional input data.

3. ANCILLARY CORRELATIONS

In the present study, following three ancillary correlations regarding P_S, ρ'' and ρ' were developed on the basis of the selected experimental data given with # in Table I.

$$\ln\frac{P_S}{P_C} = \frac{1}{1-x}\left(A_1 x + A_2 x^{1.5} + A_3 x^{2.0} + A_4 x^{4.5}\right) \tag{1}$$

$$\ln\frac{\rho''}{\rho_C} = B_1 x^{0.1} + B_2 x^{0.4} + B_3 x^{1.2} + B_4 x^{3.4} + B_5 x^{8.3} \tag{2}$$

$$\ln\frac{\rho'}{\rho_C} = C_1 x^{0.3} + C_2 x^{1.3} + C_3 x^{1.7} \tag{3}$$

Equations (1), (2) and (3) correspond to the saturation vapor-pressure, saturated vapor density and saturated liquid density, respectively. In each correlation, x=1 – T/T_C, where T_C denotes the critical temperature, 425.125 K, P_C the critical pressure, 3.796 MPa, and ρ_C the critical density, 227.84 kg·m^{-3}, as discussed in the next section, and the coefficients are listed in Table II. In our development of these correlations, we prepared a set of P_S values determined by Magee [24], and a set of ρ'' values calculated from Eq. (1) with a truncated virial equation of state with the same functional form as that we developed for R-290 [4]. It was developed based on the available $P\rho T$ property data in the vapor phase of R-600 below the critical temperature so as to generate additional ρ'' values at temperatures below 280 K where no measurements exist. It is noted that these two sets of calculated values were also used to cover the range of temperatures below

280 K and therefore Eqs. (1) through (3) are effective for temperatures from the triple point to the critical point.

4. FUNDAMENTAL EQUATION OF STATE

The developed dimensionless Helmholtz free energy, $\phi(\tau,\delta)$, model is given by Eq. (4), where the ideal-gas state contribution, $\phi^0(\tau,\delta)$, is expressed by Eq. (5) and the residual real-fluid contribution, $\phi^r(\tau,\delta)$, by Eq. (6). Independent variables are the inverse reduced temperature, $\tau = T_C/T$, and the reduced density, $\delta = \rho/\rho_C$, while f denotes the Helmholtz free energy.

$$\phi(\tau,\delta) = \frac{f}{RT} = \phi^0(\tau,\delta) + \phi^r(\tau,\delta) \tag{4}$$

$$\phi^0(\tau,\delta) = \ln\delta + a_1^0 + a_2^0\tau + a_3^0 \ln\tau + \sum_{i=4}^{7} a_i^0 \ln\left[1-\exp(-n_i\tau)\right] \tag{5}$$

$$\begin{aligned}\phi^r(\tau,\delta) = &\sum_{i=1}^{8} a_i \tau^{t_i}\delta^{d_i} + \sum_{i=9}^{13} a_i \tau^{t_i}\delta^{d_i}\exp(-\delta) \\ &+ \sum_{i=14}^{16} a_i \tau^{t_i}\delta^{d_i}\exp(-\delta^2) + \sum_{i=17}^{19} a_i \tau^{t_i}\delta^{d_i}\exp(-\delta^3)\end{aligned} \tag{6}$$

In the present model, T_C=425.125 K, ρ_C=227.85 kg·m^{-3} and P_C=3.796 MPa determined by Haynes and Goodwin [23] are used as reducing parameters, and R is the gas constant for R-600 being $R = R_m/M$ where the universal gas constant, R_m = 8.314471 J•mol^{-1}•K^{-1} [25], and the molar mass, M = 58.1234 g•mol^{-1} [26], are adopted.

The coefficients of $\phi^0(\tau,\delta)$ are listed in Table III. In Eq. (5), the first term of $\ln\delta$ is related to the ideal-gas law, and the coefficients a_1^0 and a_2^0 are determined in accord with the reference values of specific enthalpy and specific entropy for the saturated liquid at T_0 = 273.15 K, i.e., $h'(T_0)$ = 200 kJ·kg^{-1} and $s'(T_0)$ = 1.0 kJ·kg^{-1}·K^{-1}, respectively. The ideal-gas heat capacity, C_P^0, values determined by Chen et al. [27] are

reproduced within ±0.04 % by Eq. (5) for temperatures from 50 to 1500 K.

The numerical constants of the residual real-fluid contribution, $\phi^{r}(\tau,\delta)$, are also listed in Table IV. To determine the formulation of $\phi^{r}(\tau,\delta)$, we have used the programs by Tillner-Roth [28] which contain two algorithms; the Wagner's linear stepwise regression analysis for determining the structure including the combination of terms with an aid of the statistical parameters regarding the input data, and the nonlinear fitting process for adjusting the coefficients, a_i, to the data of any thermodynamic properties simultaneously. Note also that the applicability of the determined structure of the present model to other hydrocarbons including R-290 and R-600a were examined frequently in this procedure. The present model is developed on the basis of ITS-90, and the range of validity of Eq. (4) covers temperatures from 134.87 K (triple point) to 589 K, pressures up to 69 MPa and densities up to 745 kg·m^{-3}.

5. COMPARISON WITH EXPERIMENTAL DATA

Pressure deviations of available *PρT* property measurements in the vapor phase from the present model are shown in Fig. 3, while density deviations in the liquid phase are given in Fig. 4. Regarding the vapor phase, the measurements by Gupta and Eubank [11] are well represented within ±0.17 % in pressure, whereas the data by Olds et al. [9] agree with Eq. (4) within ±0.52 % in pressure as shown in Fig. 3. The *PρT* data of Beattie et al. [7] and Kay [8], which were not used as input data, are represented within ±0.87 % in pressure. In the liquid phase, the accurate *PρT* data of Haynes [10] are represented within ±0.26 % in density, while the data by Olds et al. [9] agree with Eq. (4) within ±0.49 % in density as shown in Fig. 4. The unused *PρT* data of Beattie et al. [7] and Kay [8] are represented within ±0.91 % in density except two data points of Kay [8] near the critical density.

Figure 5 shows the relative deviations of experimental C_V and W data from Eq. (4). For our smooth discussion, the relative deviations of saturated-liquid heat capacity, $C_.$,

data and saturated-liquid speed of sound, W', data were also included in Fig. 5 in which the symbol M given as an ordinate denotes these arbitrary properties. It is clear that most of those available measurements for caloric and acoustic properties of R-600 are satisfactorily represented within ±2.0 % in the effective range of the present model. In the vapor phase, the W data by Ewing et al. [15] are well represented within ±0.11 %. The C_P data in the vapor phase by Sage et al. [13] are found obsolete because of the strong systematic deviations up to −9.2 % from the present model which were not shown in Fig. 5. On the other hand, the C_V data in the liquid phase by Magee and Lüddecke [12] are represented within ±1.3 % except six data points at lower temperatures below 168 K, and the $C_{\cdot}$ data by the authors [12] are reasonably represented within ±0.52 % at temperatures 139-317 K. As shown in Fig. 5, the W data in the liquid phase by Niepmann [14] are represented within ±1.4 %, whereas the W' data by the author [14] are represented within ±0.89 %.

The comparisons of essential thermodynamic properties along the saturation boundary with the present model are shown in Fig. 6 where the symbol X given as an ordinate stands for these arbitrary properties along the saturation boundary. The calculated values from three ancillary correlations regarding P_S, ρ'' and ρ' given in Eqs. (1) through (3) are represented within ±1.0% in the range of validity of the present correlations except the ρ'' values near the triple point temperature, as clearly seen in Fig. 6. The present model represents the P_S measurements by Flebbe et al. [16] and Kratzke et al. [17] within ±0.084 %, while the calculated P_S values at lower temperatures by Magee [24] agree with the present equation of state within ±0.82 % (±0.2 kPa). As shown in Fig. 6, the ρ'' data of Olds et al. [9] and Sliwinski [19] are represented within ±0.39 % except a single datum of each series, while the ρ' data by Sliwinski [19], McClune [20], Haynes and Hiza [21], and Orrit and Laupretre [22] are well represented within ±0.15 %. A significant deviation of ρ'' and ρ' data of Kay [8] can also be observed in Fig. 6.

As one of the most important tests for the accuracy of the thermodynamic model, moreover, the behaviors of C_V and C_P over an extended range of temperatures and pressures are demonstrated in Figs. 7 and 8, respectively. From the physically reasonable behaviors shown in both figures in the entire range including the extrapolated region where no experimental data are available, it is confirmed that the present model does exhibit a satisfactory thermodynamic consistency in the entire fluid phase of R-600.

6. CONCLUSION

We developed the equation of state for R-600 which is valid for temperatures from 134.87 K (the triple point temperature) to 589 K, pressures up to 69 MPa, and densities up to 745 kg·m^{-3}. The accurate experimental thermodynamic property data of R-600 are satisfactorily represented, and the smooth behaviors of the calculated isochoric and isobaric heat capacity values have also been confirmed in the range of validity of the present model.

ACKNOWLEDGMENTS

The authors are grateful to Dr. J. W. Magee who kindly provided his unpublished data which were useful for our study.

REFERENCES

1. R. Tillner-Roth and A. Yokozeki, *J. Phys. Chem. Ref. Data* **26**:1273 (1997).
2. R. Tillner-Roth and H. D. Baehr, *J. Phys. Chem. Ref. Data* **23**:657 (1994).
3. E. W. Lemmon and R. T. Jacobsen, paper to be appeared in *J. Phys. Chem. Ref. Data* (2000).
4. H. Miyamoto and K. Watanabe, paper to be submitted to *Int. J. Thermophys.* (2000).
5. B. A. Younglove and J. F. Ely, *J. Phys. Chem. Ref. Data* **16**:577 (1987).
6. M. O. McLinden, S. A. Klein, E. W. Lemmon, and A. P. Peskin, *NIST Thermodynamic and Transport Properties of Refrigerants and Refrigerant Mixtures (REFPROP)* Ver. 6.01: (U.S. Dept. Commerce, Washington, 1998).
7. J. A. Beattie, G. L. Simard, and G.-J. Su, *J. Am. Chem. Soc*. **61**:26 (1939).
8. W. B. Kay, *Ind. Eng. Chem*. **32**:358 (1940).
9. R. H. Olds, H. H. Reamer, B. H. Sage, and W. N. Lacey, *Ind. Eng. Chem*. **36**:282 (1944).
10. W. M. Haynes, *J. Chem. Thermodyn*. **15**:801 (1983).
11. D. Gupta and P. T. Eubank, *J. Chem. Eng. Data* **42**:961 (1997).
12. J. W. Magee and T. O. D. Lüddecke, *Int. J. Thermophys*. **19**:129 (1998).
13. B. H. Sage, D. C. Webster, and W. N. Lacey, *Ind. Eng. Chem*. **29**:1309 (1937).
14. R. Niepmann, *J. Chem. Thermodyn*. **16**:851 (1984).
15. M. B. Ewing, A. R. H. Goodwin, M. L. McGlashan, and J. P. M. Trusler, *J. Chem. Thermodyn*. **20**:243 (1988).
16. J. L. Flebbe, D. A. Barclay, and D. B. Manley, *J. Chem. Eng. Data* **27**:405 (1982).
17. H. Kratzke, E. Spillner, and S. Müller, *J. Chem. Thermodyn*. **14**:1175 (1982).
18. W. D. Machin and P. D. Golding, *J. Chem. Soc., Faraday. Trans*. **85**:2229 (1989).
19. P. Sliwinski, *Z. Phys. Chemie. Neue Folge* **63**:263 (1969).
20. C. R. McClune, *Cryogenics* **16**:289 (1976).
21. W. M. Haynes and M. J. Hiza, *J. Chem. Thermodyn*. **9**:179 (1977).

22. J. E. Orrit and J. M. Laupretre, *Adv. Cryog. Eng*. **23**:573 (1978).

23. W. M. Haynes and R. D. Goodwin, NBS Monograph 169, (U.S. Dept. Commerce, Washington, 1982), p.197.

24. J. W. Magee, New information for the saturation vapor-pressure of lower temperatures was provided as private communication (1999).

25. M. R. Moldover, J. P. M. Trusler, T. J. Edwards, J. B. Mehl, and R. S. Davis, *J. Res. Natl. Bur. Stand.* **93**:85 (1988).

26. IUPAC Commission on Atomic Weights and Isotopic Abundances, *J. Phys. Chem. Ref. Data* **24**:1561 (1995).

27. S. S. Chen, R. C. Wilhoit, and B. J. Zwolinski, *J. Phys. Chem. Ref. Data* **4**:859 (1975).

28. R. Tillner-Roth, Several programs for the modeling were provided as private communication (1996).

Table I. Experimental Thermodynamic Property Data for R-600

First author[1)]	Ref.	Property	No. of Data	P		ρ		T	
				Range (MPa)	δP [2)] (%)	Range ($kg \cdot m^{-3}$)	$\delta\rho$ ($kg \cdot m^{-3}$)	Range (K)	δT [2)] (mK)
Beattie	[7]	$P\rho T$	116	1.5–36	n.a.	29–494	n.a.	423–573	n.a.
Kay	[8]	$P\rho T$	453	0.2–8.3	0.4	4.6–513	0.15 %	311–589	60
Olds#	[9]	$P\rho T$	217	0.1–69	0.1	0.9–632	0.10 %	311–511	6
Haynes#	[10]	$P\rho T$	105	1.7–36	0.01	572–745	0.10 %	140–300	10 (30)
Gupta#	[11]	$P\rho T$	49	0.0–1.1	n.a.	0.4–19	n.a.	265–450	n.a.
Magee#	[12]	C_V	148	1.9–33	n.a.	546–720	n.a.	153–342	n.a.
Sage	[13]	C_P	8	0.1	0.1			294–411	60
Niepmann#	[14]	W	230	0.1–60	n.a.			200–375	n.a.
Ewing#	[15]	W	78	0.0–0.1	n.a.			250–320	n.a.
Kay	[8]	P_S	20	0.5–3.8	0.4			325–425	60
Flebbe#	[16]	P_S	12	0.1–1.1	0.015 (100 Pa)			278–358	7
Kratzke#	[17]	P_S	12	0.5–3.7	0.03			320–423	10
Machin	[18]	P_S	224	0.0–0.1	0.06 (0.3 Pa)			173–280	2
Kay	[8]	ρ''	20			13–228	0.15 %	325–425	60
Olds#	[9]	ρ''	4			8.9–97	0.10 %	311–411	6
Sliwinski#	[19]	ρ''	10			4.0–35	0.05	283–368	n.a.
Kay	[8]	ρ'	20			228–541	0.15 %	325–425	60
Olds	[9]	ρ'	4			372–557	0.10 %	311–411	6
Sliwinski#	[19]	ρ'	10			476–590	0.05	283–368	n.a.
McClune#	[20]	ρ'	7			700–727	0.10 %	143–173	100
Haynes#	[21]	ρ'	12			570–735	0.10 %	135–300	40
Orrit#	[22]	ρ'	50			598–735	0.4	135–275	n.a.
Magee#	[12]	C_σ	100					139–317	n.a.
Niepmann#	[14]	W'	19	0.0–1.2	n.a.			200–360	n.a.

1) Data used as input data are given with #.
2) Numerical figures in parenthesis denote the maximum experimental uncertainty claimed.

Table II. Coefficients in Eqs. (1) through (3)

i	A_i	B_i	C_i
1	−7.246998	−0.04856485	1.378063
2	2.899084	−2.764049	−0.4003577
3	−2.506508	−6.323427	0.3561708
4	−2.460527	−22.60585	
5		−72.67645	

Table III. Coefficients in Eq. (5)

i	a_i^0	n_i
1	–5.404074	————
2	4.911202	————
3	3.240207	————
4	5.513671	0.7705025
5	7.38845	3.10278
6	10.25063	9.735094
7	11.06101	4.385458

Table IV. Coefficients and Exponents in Eq. (6)

i	a_i	t_i	d_i
1	2.969966×0^{-1}	–0.25	1
2	-1.327401×0^{0}	1.50	1
3	-1.709594×0^{-3}	–0.75	2
4	2.231660×0^{-1}	0.00	2
5	-3.604211×0^{-2}	1.25	3
6	1.896994×0^{-3}	1.50	5
7	7.321336×0^{-5}	0.50	8
8	-1.396499×0^{-6}	2.50	8
9	-2.508606×0^{0}	1.50	3
10	2.401618×0^{0}	1.75	3
11	1.437078×0^{-3}	–0.25	8
12	-9.520527×0^{-3}	3.00	5
13	2.644955×0^{-3}	3.00	6
14	-1.980616×0^{-1}	4.00	1
15	-3.752346×0^{-2}	2.00	5
16	1.632013×0^{-3}	–1.00	7
17	-2.361746×0^{-2}	2.00	2
18	-9.432051×0^{-3}	19.00	3
19	3.880739×0^{-5}	5.00	15

FIGURE CAPTIONS

Fig. 1. Distribution of experimental $P\rho T$ property data.

□: Beattie et al. [7] Δ: Kay [8] *: Olds et al. [9]

×: Haynes [10] ○: Gupta and Eubank [11]

Fig. 2. Distribution of caloric and acoustic property data.

□: (C_P), Sage et al. [13] ×: (W), Niepmann [14] Δ: (W), Ewing et al. [15]

•: (C_V), Magee and Lüddecke [12]

Fig. 3. Pressure deviations of $P\rho T$ property data from Eq. (4).

□: Beattie et al. [7] −: Kay [8] *: Olds et al. [9]

•: Gupta and Eubank [11]

Fig. 4. Density deviations of $P\rho T$ property data from Eq. (4).

□: Beattie et al. [7] −: Kay [8] *: Olds et al. [9] ×: Haynes [10]

Fig. 5. Deviations of various caloric and acoustic property data from Eq. (4).

×: (W), Niepmann [14] Δ: (W), Ewing et al. [15]

•: (C_V), Magee and Lüddecke [12] *: (W'), Niepmann [14]

•: ($C_.$), Magee and Lüddecke [12]

Fig. 6. Deviations of measured and calculated P_S, ρ'' and ρ' values from the present model.

P_S; Δ: Kay [8] □: Flebbe et al. [16] •: Kratzke et al. [17] •:Machin and Golding (additional two data points: +18.3 %, −19.5 %) [18]

•: Magee [24] ••: Eq. (1)

ρ''; Δ: Kay [8] •: Olds et al. [9] •: Sliwinski [19] - - - -: Eq. (2)

ρ'; Δ: Kay [8] •: Olds et al. [9] •: Sliwinski [19] +: McClune [20]

□: Haynes and Hiza [21] *: Orrit and Laupretre [22] — −: Eq. (3)

Fig. 7. Calculated isochoric heat capacity values along isobars from the present model.

Fig. 8. Calculated isobaric heat capacity values along isobars from the present model.

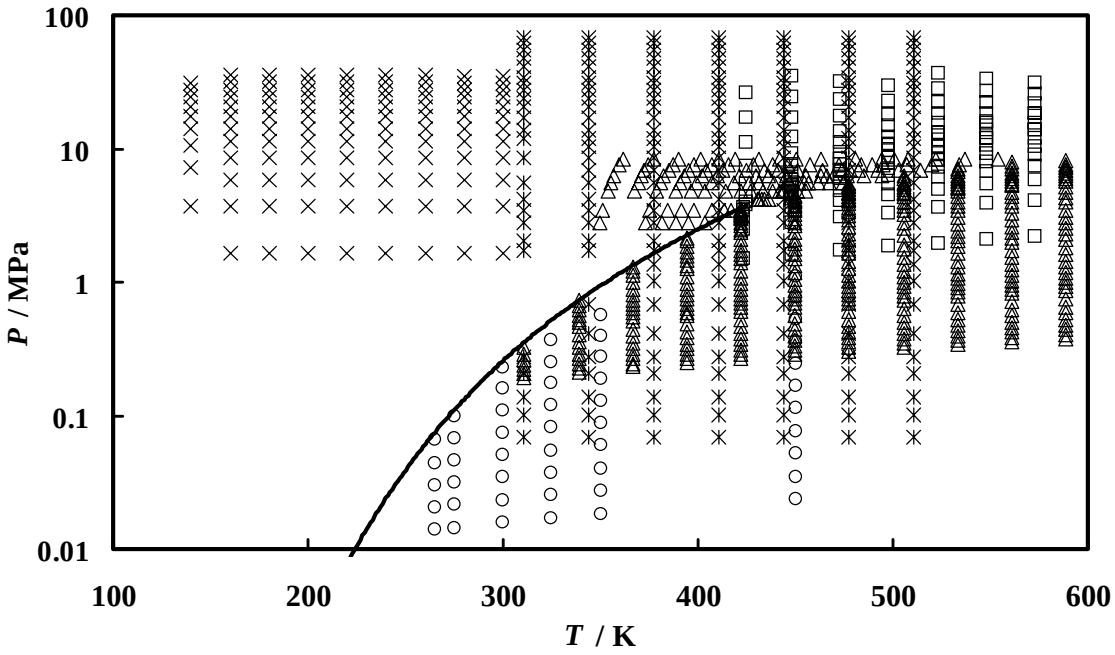

H. Miyamoto and K. Watanabe Figure 1

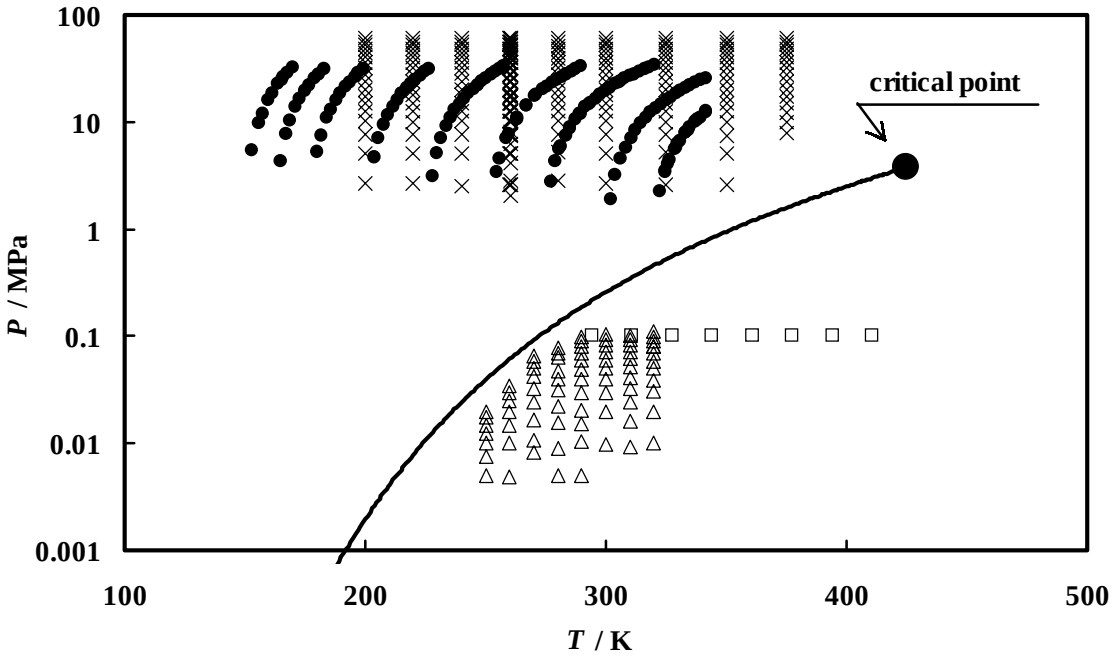

H. Miyamoto and K. Watanabe Figure 2

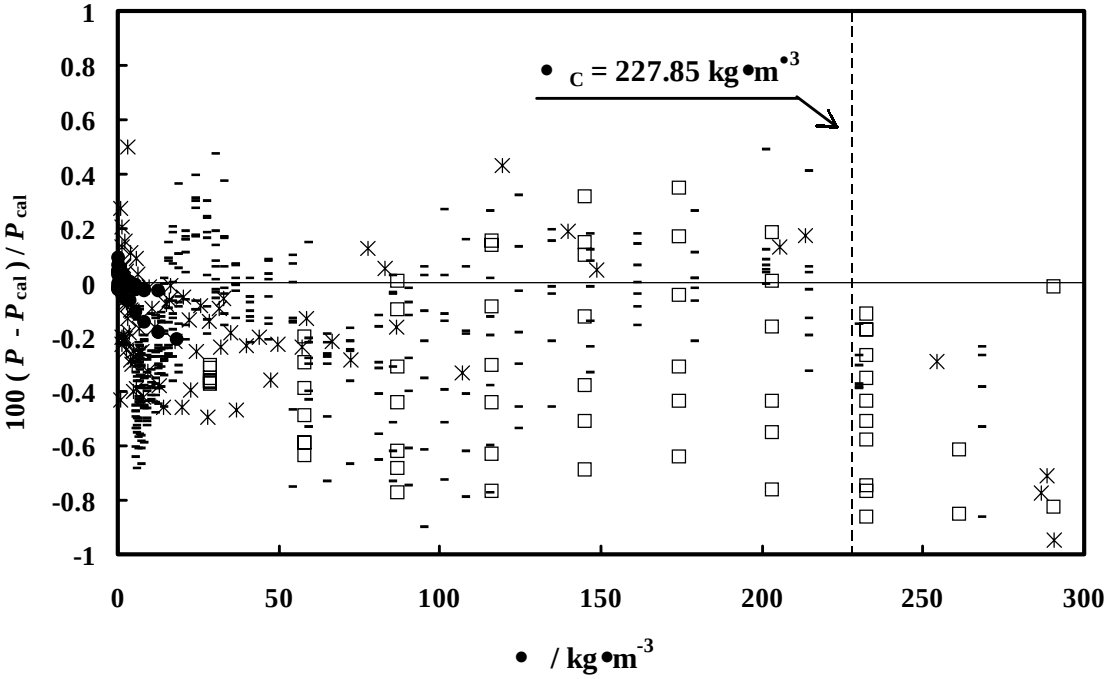

H. Miyamoto and K. Watanabe Figure 3

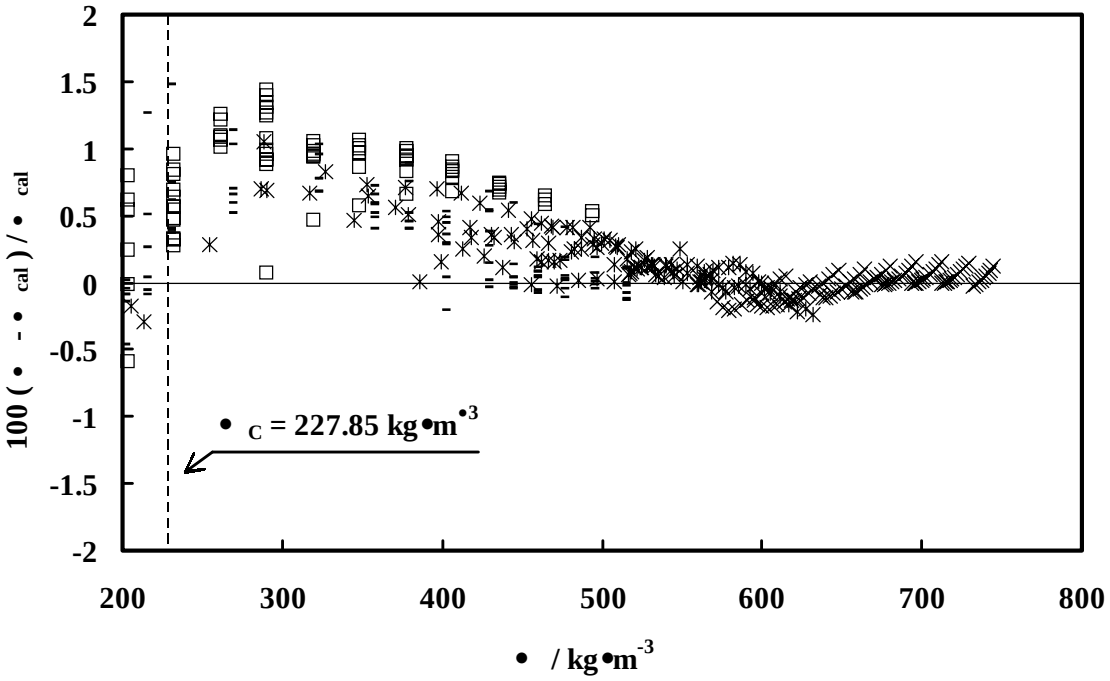

H. Miyamoto and K. Watanabe Figure 4

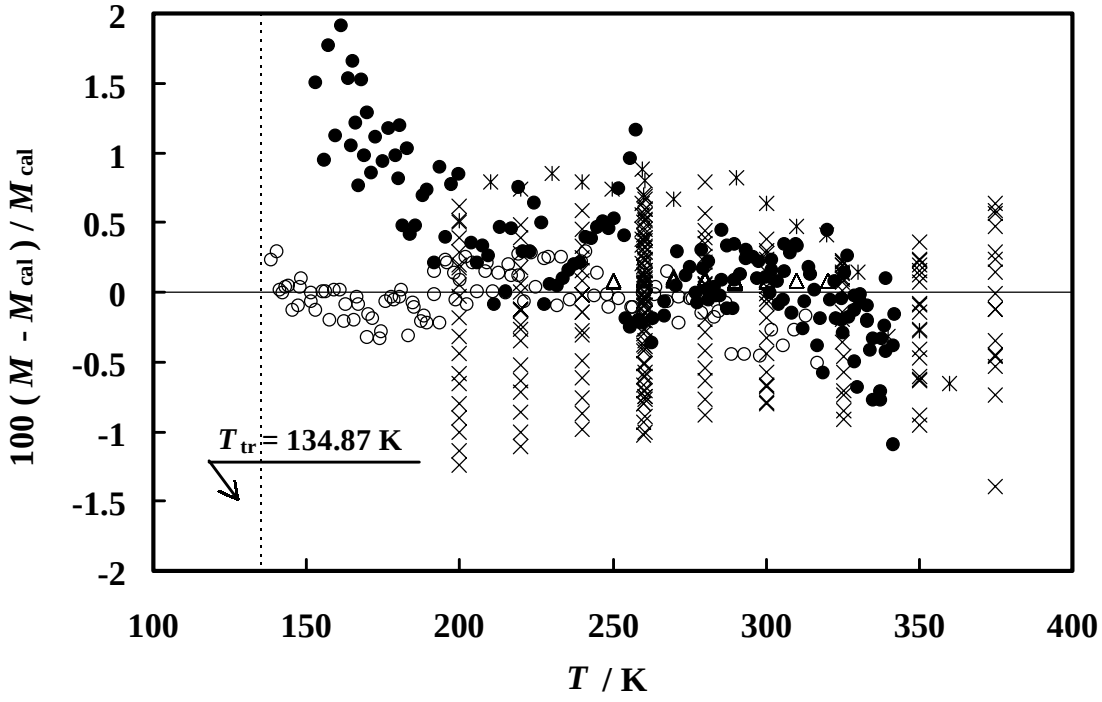

H. Miyamoto and K. Watanabe Figure 5

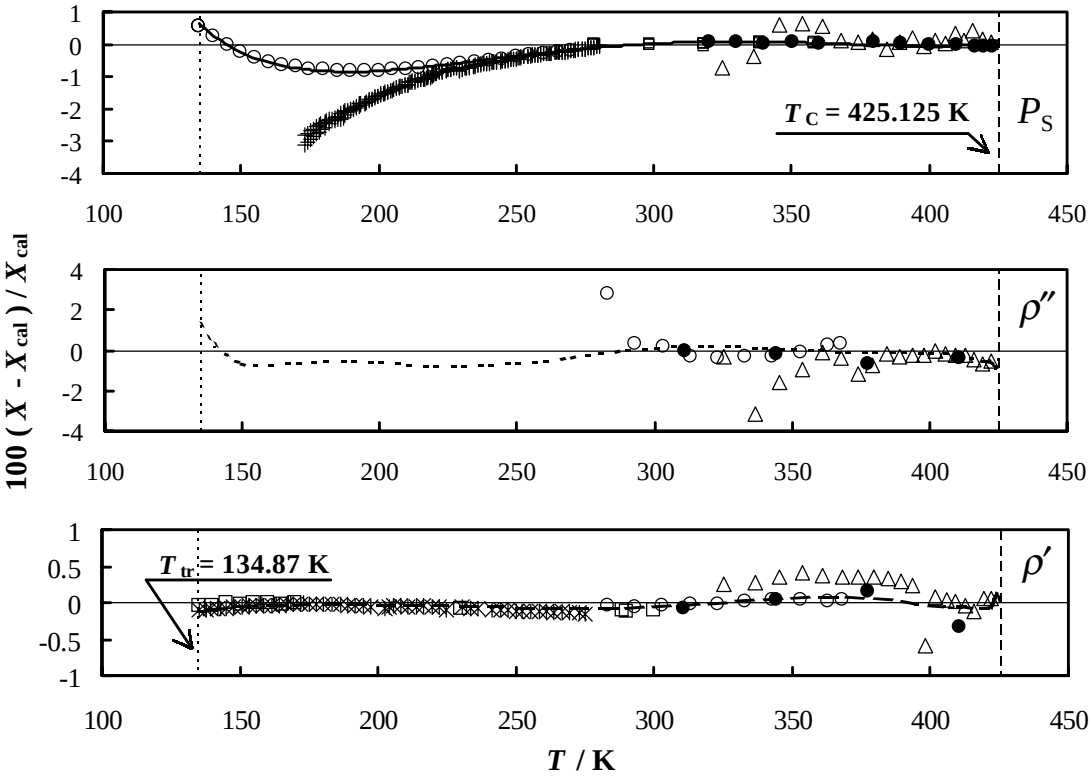

H. Miyamoto and K. Watanabe Figure 6

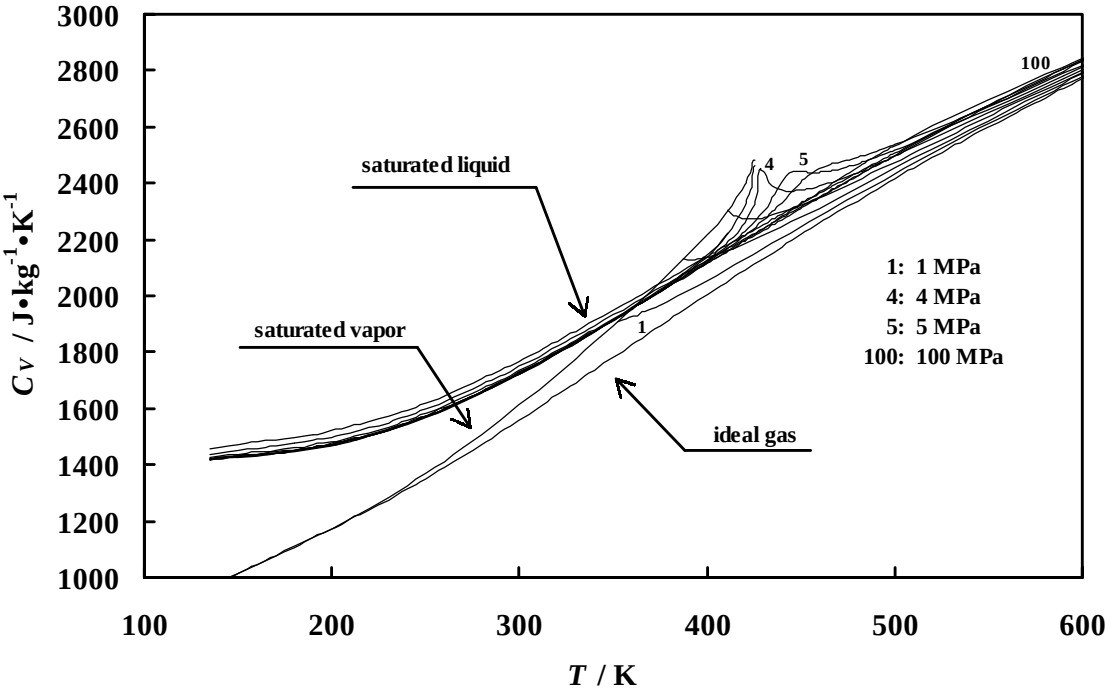

H. Miyamoto and K. Watanabe Figure 7

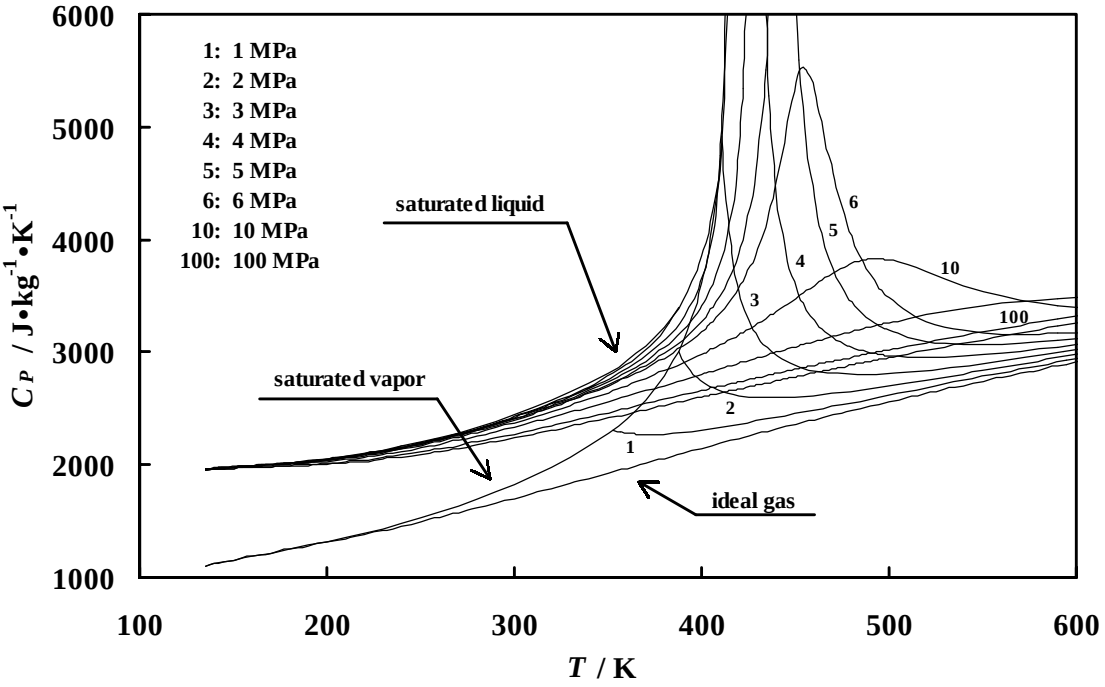

H. Miyamoto and K. Watanabe Figure 8